

# Order and Surface Processes in III-V Semiconductor Alloys

G.B. Stringfellow

## Introduction

Semiconductor alloys have become increasingly useful during the last four decades because, through the use of alloys, the properties of semiconductors can be tailored by varying the composition to precisely match the requirements for specific electronic and photonic devices. In addition the use of alloys allows the production of special structures, such as quantum wells, that require rapid changes in bandgap energy during growth. This has led to so-called "band-gap engineering," in which device designers and epitaxial growers are working together to produce structures having virtually atomic-scale dimensions.

Most compound semiconductors crystallize in the zinc-blende structure, which consists of two interpenetrating face-centered-cubic (fcc) sublattices, one for the anions and one for the cations. Each atom is surrounded by four neighbors, as in the diamond cubic lattice, to facilitate the largely covalent  $sp^3$  bonding typical of semiconductor materials. Compound semiconductor alloys of the type  $A_xB_{1-x}C$  are often considered to consist of a random arrangement of A and B atoms on one fcc sublattice. However real alloys are nearly always nonrandom.

One type of deviation from randomness involves clustering of like atoms, a familiar phenomenon in materials with miscibility gaps. In an extreme case, this leads to phase separation—that is, the formation of distinct AC- and BC-rich phases. The two physically distinct phases formed are easily observed using, for example, x-ray diffraction or microscopic observation of the structure.

Another deviation from randomness is order. In an ordered crystal, the solid composition is modulated along a par-

ticular crystallographic direction with a period of several lattice spacings. This results in formation of natural, monolayer superlattice structures in semiconductor alloys, which has important consequences for the optical and electrical properties. In the extreme case of perfect

order, an alloy of the type  $A_xB_{1-x}C$ , with mixing of A and B atoms on the cation sublattice, might order to produce alternating layers of pure AC and pure BC. The alloy could also be of the type  $AC_xD_{1-x}$ , with mixing on the anion sublattice, where perfect ordering would produce alternating AC and AD layers. Both phase separation and ordering were observed in metal systems many decades ago and were more recently discovered to occur spontaneously during growth of semiconductor alloys.<sup>1-5</sup>

Three common types of order are observed in III-V alloys with a 1:1 ratio of the two constituent binary compounds. The most frequently observed form for these alloys grown epitaxially on (001) oriented substrates is the rhombohedral CuPt structure, with ordering on one or two of the set of four {111} planes. Ordering on the ( $\bar{1}\bar{1}\bar{1}$ ) and ( $1\bar{1}\bar{1}$ ) planes (the B variants) is referred to as CuPt-B, and CuPt-A refers to ordering on the other two {111} planes (the A variants). A summary of the particular ordered structures seen for various alloys appears in Table I. The tetragonal CuAu structure, with ordering on the set of {100} planes,

Table I: Summary of Ordering Observed in Semiconductor Alloys (After Stringfellow and Chen<sup>6</sup>).

Material	Growth Technique	Substrate Orientation	Ordered Structure
AlGaAs	OMVPE & MBE	(110)	CuAu
GaAsSb	OMVPE	(110)	CuAu
GaInAs	MBE	(110)	CuAu
GaAsSb	OMVPE	(001)	CuAu+CH
GaAsSb	MBE	(001)	CH+CuPt
GaInAsSb	OMVPE	(001)	CuAu+CH
AlGaInP	OMVPE	(001)	CuPt-A+B
AlInP	OMVPE	(001)	CuPt
AlInAs	MBE	(001)	CuPt
GaAsP	OMVPE	(001)	CuPt-B
GaAsSb	MBE	(001)	CuPt-B
GaAsSb	MBE	(001)	CuPt-B
GaInAs	OMVPE	(001)	CuPt
GaInAs	VLE	(001)	CuPt
GaInAsP	VLE	(001)	CuPt
GaInAsP	OMVPE	(001)	CuPt
GaInP	OMVPE	(001)	CuPt-B
GaInSb	OMVPE	(001)	CuPt
InAsSb	OMVPE	(001)	CuPt
InAsSb	MBE	(001)	CuPt
InPSb	OMVPE	(001)	CuPt

OMVPE = organometallic vapor-phase epitaxy, MBE = molecular-beam epitaxy, VLE = vapor levitation epitaxy.

has also been observed for several III-V alloys, particularly for growth on {110} oriented substrates, as Table I shows.<sup>1,2,5,6</sup> Ironically the rarest structure, the chalcopyrite (CH) structure with ordering on {210} planes, is also predicted to be the most stable in the bulk alloys.<sup>8,9</sup> This is because the ordered structure formed is the most thermodynamically stable *at the surface*. It need not be the most thermodynamically stable in the bulk, as will be discussed in detail. Ordering in semiconductor alloys is not restricted to the III-V systems. The formation of similar {111} ordered structures has been reported for II-VI alloys<sup>9</sup> and for Si-Ge alloys.<sup>10</sup>

The simplest indicator of the occurrence of ordering is the observation of extra spots in the transmission-electron-diffraction (TED) pattern. For example, for ordered structures with a spacing twice the normal lattice spacing, extra superspots are observed in the TED patterns with spacings of precisely one-half of those for the normal zinc-blende lattice. An example appears in Figure 1. The [001]-pole electron-diffraction pattern in Figure 1a is for an (001)-oriented, disordered layer of GaAs<sub>0.5</sub>Sb<sub>0.5</sub> grown by organometallic vapor-phase epitaxy (OMVPE). It shows only the diffraction spots observed in a binary compound, such as GaAs, with the zinc-blende structure. The [001]-pole electron-diffraction pattern in Figure 1b is for an (001)-oriented, ordered layer of GaAs<sub>0.5</sub>Sb<sub>0.5</sub>, also grown by OMVPE but using different conditions. It exhibits an array of extra spots at positions halfway between the spots due to the sets of {100} and {210} lattice planes. Figures 1c and 1d are the [110]-pole electron-diffraction patterns for Ga<sub>0.5</sub>In<sub>0.5</sub>P layers, also grown by OMVPE. Figure 1c shows a disordered layer, and Figure 1d is for an ordered layer. The latter shows extra superlattice spots at positions halfway from the origin to the spots due to the {111} planes in the zinc-blende lattice. The diffraction pattern in Figure 1b shows the existence of two ordered structures, the CuAu and CH structures, within the area probed by the electron beam. The diffraction pattern in Figure 1d indicates the existence of the B variants of the CuPt structure in the Ga<sub>0.5</sub>In<sub>0.5</sub>P layer.

The degree of order is typically significantly less than unity. For samples with large domains, TED superspot-intensity measurements yield values of degree of order as large as 0.7.<sup>11</sup> Recent spin-echo nuclear-magnetic-resonance measurements of <sup>71</sup>Ga<sup>12</sup> yield the best independent value to date of 0.6 for a sample grown to maximize the order parameter.

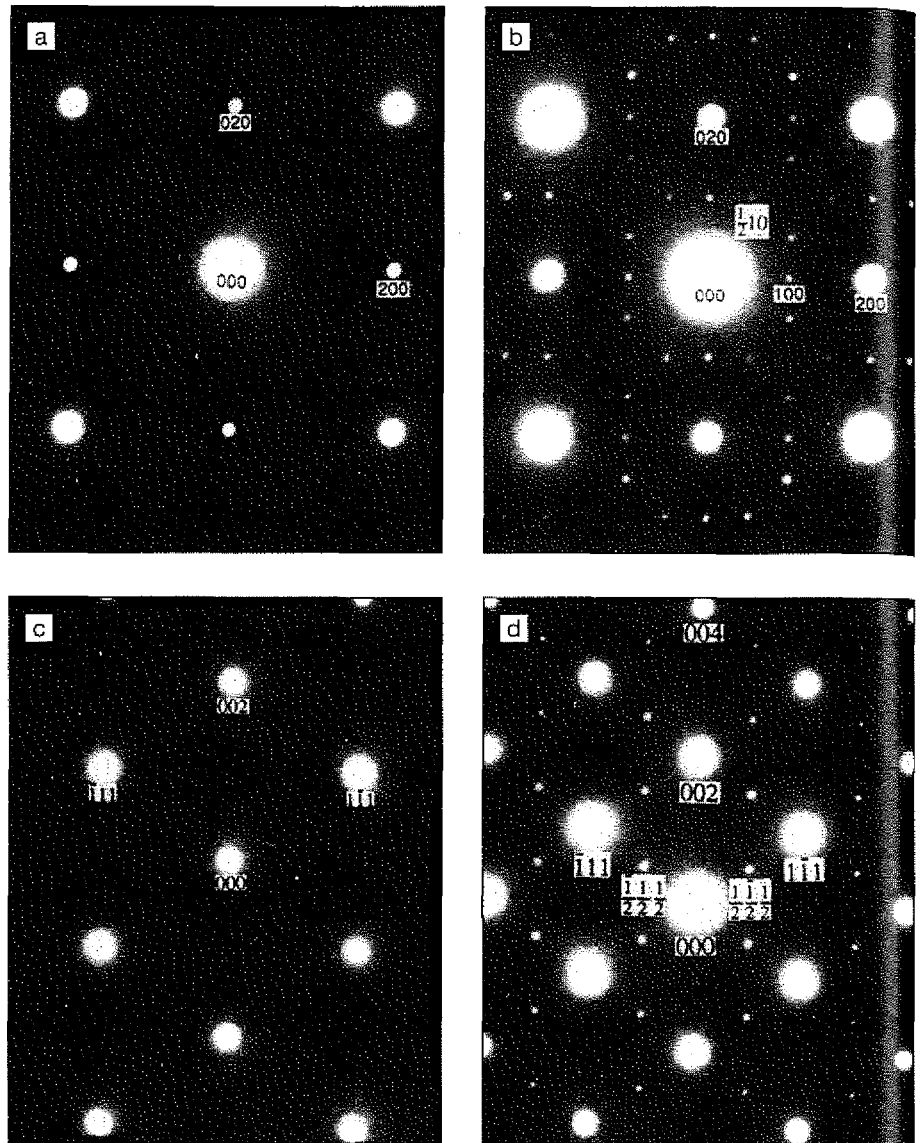


Figure 1. Transmission-electron-diffraction (TED) patterns of semiconductor alloys. [001]-pole TED patterns of disordered (a) and ordered (b) GaAsSb, and [110]-pole TED patterns of disordered (c) and ordered (d) GaInP.

Optical properties are often used to estimate the degree of order. Most commonly this involves the use of low-temperature photoluminescence to determine the bandgap energy and the use of theoretical calculations to extract the degree of order. This type of analysis leads to a value of 0.56 for the order parameter in highly ordered GaInP grown by OMVPE.<sup>13</sup> A comparison of the values of order parameter obtained from the various techniques shows a high degree of consistency, providing support for the idea that the maximum degree of order obtained is 0.5–0.6. The disorder may be

due to two factors: (1) regions of the material that are not ordered<sup>14</sup> and (2) a compositional modulation index of less than unity—that is, the alternating monolayers are not really the pure compounds from which the alloy is formed.

The occurrence and mechanism of ordering are fascinating materials-science problems that reveal much about the thermodynamics and structure-properties relationships for semiconductor alloys. They are also beginning to reveal important general features of the surface processes occurring during vapor-phase-epitaxial (VPE) growth. Ordering also

has also been observed for several III-V alloys, particularly for growth on  $\{110\}$  oriented substrates, as Table I shows.<sup>1,2,5,6</sup> Ironically the rarest structure, the chalcopyrite (CH) structure with ordering on  $\{210\}$  planes, is also predicted to be the most stable in the bulk alloys.<sup>8,9</sup> This is because the ordered structure formed is the most thermodynamically stable *at the surface*. It need not be the most thermodynamically stable in the bulk, as will be discussed in detail. Ordering in semiconductor alloys is not restricted to the III-V systems. The formation of similar  $\{111\}$  ordered structures has been reported for II-VI alloys<sup>9</sup> and for Si-Ge alloys.<sup>10</sup>

The simplest indicator of the occurrence of ordering is the observation of extra spots in the transmission-electron-diffraction (TED) pattern. For example, for ordered structures with a spacing twice the normal lattice spacing, extra superspots are observed in the TED patterns with spacings of precisely one-half of those for the normal zinc-blende lattice. An example appears in Figure 1. The  $[001]$ -pole electron-diffraction pattern in Figure 1a is for an  $(001)$ -oriented, disordered layer of  $\text{GaAs}_{0.5}\text{Sb}_{0.5}$  grown by organometallic vapor-phase epitaxy (OMVPE). It shows only the diffraction spots observed in a binary compound, such as GaAs, with the zinc-blende structure. The  $[001]$ -pole electron-diffraction pattern in Figure 1b is for an  $(001)$ -oriented, ordered layer of  $\text{GaAs}_{0.5}\text{Sb}_{0.5}$ , also grown by OMVPE but using different conditions. It exhibits an array of extra spots at positions halfway between the spots due to the sets of  $\{100\}$  and  $\{210\}$  lattice planes. Figures 1c and 1d are the  $[110]$ -pole electron-diffraction patterns for  $\text{Ga}_{0.5}\text{In}_{0.5}\text{P}$  layers, also grown by OMVPE. Figure 1c shows a disordered layer, and Figure 1d is for an ordered layer. The latter shows extra superlattice spots at positions halfway from the origin to the spots due to the  $\{111\}$  planes in the zinc-blende lattice. The diffraction pattern in Figure 1b shows the existence of two ordered structures, the CuAu and CH structures, within the area probed by the electron beam. The diffraction pattern in Figure 1d indicates the existence of the B variants of the CuPt structure in the  $\text{Ga}_{0.5}\text{In}_{0.5}\text{P}$  layer.

The degree of order is typically significantly less than unity. For samples with large domains, TED superspot-intensity measurements yield values of degree of order as large as 0.7.<sup>11</sup> Recent spin-echo nuclear-magnetic-resonance measurements of  $^{71}\text{Ga}$ <sup>12</sup> yield the best independent value to date of 0.6 for a sample grown to maximize the order parameter.

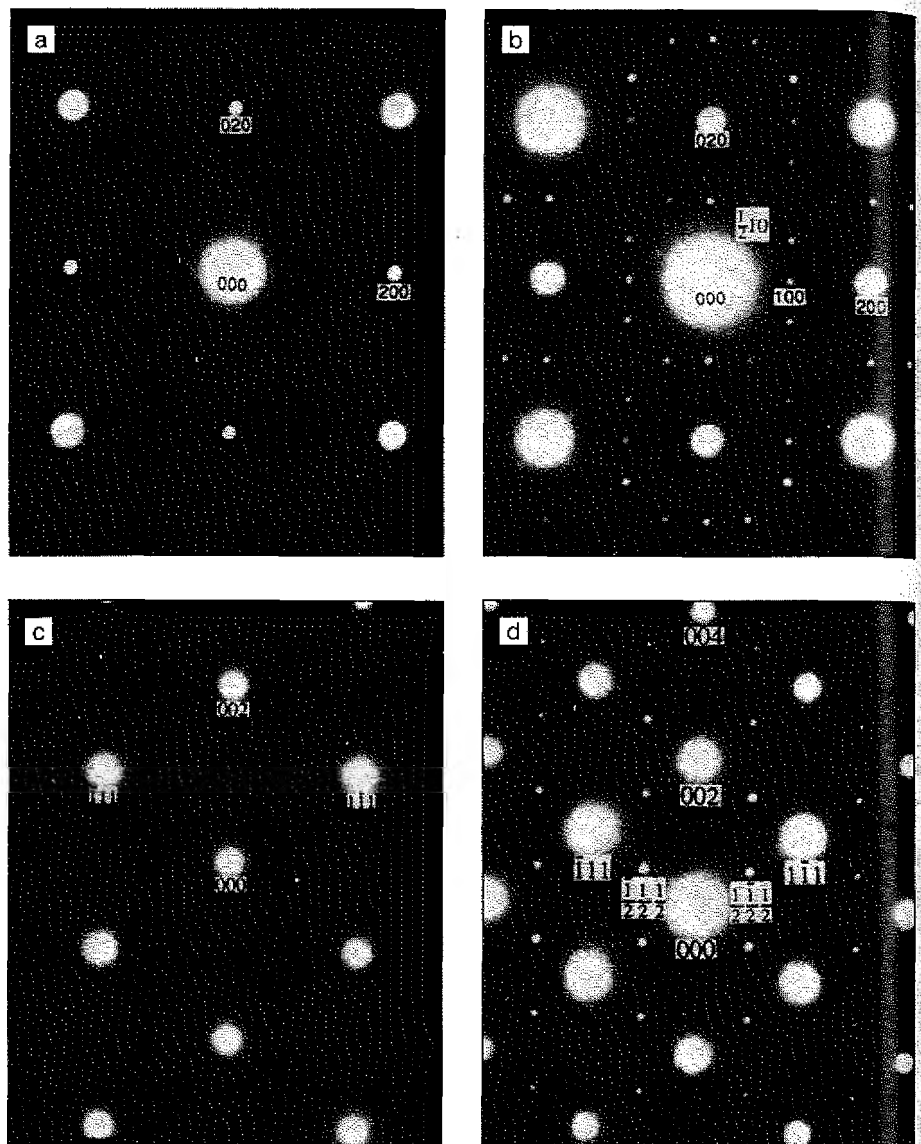


Figure 1. Transmission-electron-diffraction (TED) patterns of semiconductor alloys.  $[001]$ -pole TED patterns of disordered (a) and ordered (b)  $\text{GaAsSb}$ , and  $[110]$ -pole TED patterns of disordered (c) and ordered (d)  $\text{GaInP}$ .

Optical properties are often used to estimate the degree of order. Most commonly this involves the use of low-temperature photoluminescence to determine the bandgap energy and the use of theoretical calculations to extract the degree of order. This type of analysis leads to a value of 0.56 for the order parameter in highly ordered  $\text{GaInP}$  grown by OMVPE.<sup>13</sup> A comparison of the values of order parameter obtained from the various techniques shows a high degree of consistency, providing support for the idea that the maximum degree of order obtained is 0.5–0.6. The disorder may be

due to two factors: (1) regions of the material that are not ordered<sup>14</sup> and (2) a compositional modulation index of less than unity—that is, the alternating monolayers are not really the pure compounds from which the alloy is formed.

The occurrence and mechanism of ordering are fascinating materials-science problems that reveal much about the thermodynamics and structure-properties relationships for semiconductor alloys. They are also beginning to reveal important general features of the surface processes occurring during vapor-phase-epitaxial (VPE) growth. Ordering also

has extremely important practical consequences. The order-induced property change eliciting the most interest by the device community is the reduction of the bandgap energy. More than 10 years before ordering was discovered, an unexplained phenomenon caused the bandgap energies of GaInP layers, all grown lattice-matched to GaAs substrates—that is, all with the same composition—to vary by more than 100 meV from laboratory to laboratory.<sup>15</sup> The reduction of bandgap energy was later found to be caused by CuPt ordering.<sup>16</sup> The first attempts to quantitatively determine the effect of order on the bandgap energy were theoretical.<sup>7</sup> The current best theoretical estimate of the bandgap reduction due to CuPt ordering in perfectly ordered GaInP,  $\Delta E_g$ , is 0.38 eV.<sup>17</sup> The reduction in bandgap energy has the following dependence on the degree of order  $S$ <sup>18</sup>:

$$E_g = E_g(S = 0) - \Delta E_g S^2. \quad (1)$$

Ernst et al<sup>19</sup> examined the bandgap energy versus order parameter experimentally over a range of bandgap energies, yielding  $\Delta E_g$  of 471 meV.

Bandgap narrowing due to CuPt ordering has also been experimentally observed in GaInAs alloys lattice-matched to InP(001) substrates.<sup>20</sup> A maximum bandgap reduction of 65 meV was observed. Experimental determination of the effect of CuPt order on the bandgap of InAsSb alloys reveals a bandgap shrinkage of approximately 45 meV.<sup>21</sup>

The large bandgap shrinkage due to order in GaInP is extremely important for visible light-emitting diodes and injection laser diodes. To produce the shortest wavelength (most visible) devices, ordering must be avoided. However in InAsSb alloys, the shrinkage of bandgap energy is potentially beneficial since it moves the wavelength further into the infrared (IR) where an atmospheric window exists between 8 and 12  $\mu\text{m}$ .<sup>21</sup> Thus ordered InAsSb has the potential to be a useful material for IR detectors if ordering can be precisely controlled. An additional potential benefit of ordering is the production of order/disorder heterostructures with absolutely no change in the solid composition.<sup>22</sup>

The ordering phenomenon in semiconductor alloys is reported virtually only for alloys grown by VPE processes. As will be discussed in more detail, this is because the ordering process is driven mainly by the surface thermodynamics. The widely observed CuPt structure is stable only for the surface reconstruction(s) that form(s) [110] rows of [110]

group-V dimers on the (001) surface. These group-V-dimer rows form to reduce the energy due to the large number of dangling bonds at the surface.

This article will concentrate on (1) the driving force for ordering and (2) the effects of growth parameters on the ordering process. These topics are important because they lead to a better understanding of the mechanism leading to ordering and to the control of the ordering process.

### Thermodynamic Driving Force for Ordering

The simplest model to describe the thermodynamics of mixing in any alloy system is the ideal solution model where the distribution of constituents is random and the enthalpy of mixing is zero. For many materials systems, deviations from ideal behavior are accounted for using the regular solution model.<sup>23</sup> In this model, the entropy of mixing is considered to be equal to the ideal configurational entropy of mixing, which always favors the formation of random alloys. The enthalpy of mixing is given by the symmetrical function  $\Delta H^M(x) = \Omega x(1-x)$  where  $\Omega$  is the interaction parameter related in the regular solution model to the relative energies of AB, AA, and BB "bonds" in the alloy  $A_xB_{1-x}C$ . A positive interaction parameter indicates that AB bonds have a higher energy than the average of AA and BB bonds. This is an indicator that clustering and phase separation may occur at low temperatures where entropy is not the dominant term in the total free energy. In the regular solution model, a negative value of the interaction parameter indicates that A and B atoms are attracted to each other. This gives rise to ordering.

The regular solution model does not appear to be fundamentally suited to the description of the thermodynamics of mixing in compound semiconductor alloys since for example the Ga and Al do not form bonds in AlGaAs alloys. Another general drawback to the regular solution model is that it is not predictive. The interaction parameters for the liquid and the solid phases are adjustable constants, typically obtained by fitting the calculated solid/liquid phase diagram to the experimental data.

An attempt to produce a model more physically reasonable and more predictive led to the delta-lattice-parameter (DLP) mode.<sup>23,24</sup> In this model, the enthalpy of mixing for a semiconductor alloy is related to the effect of composition on the total energy of the bonding electrons. This leads to an approximate representation of the interaction parameter

in terms of only the lattice parameters of the two binary constituents of the ternary alloy,<sup>24</sup>

$$\Omega = 4.375 K(\Delta a)^2/\bar{a}^{4.5}. \quad (2)$$

In this equation,  $\Delta a$  is the lattice-parameter difference, and  $\bar{a}$  is the average lattice parameter. The adjustable constant is  $K$ , which is the same for all III-V alloys. Thus once  $K$  has been established for one or more alloys, this expression can be used to predict the values of interaction parameter for other alloys. This simple model gives values of interaction parameter that are in remarkably good agreement with experimental data.<sup>24,25</sup> It is also more physical and predictive.

A major prediction of the DLP model is that the values of  $\Omega$  are always greater than or equal to zero. This means in the regular-solution view that the solid III-V alloys may cluster and phase-separate, but they will not order. The  $\Delta a^2$  dependence in Equation 2 suggests that the main effect in the DLP model is the strain energy associated with deformation of the bonds in the alloy. Thus the valence-force-field (VFF) model, originally developed by Keating,<sup>26</sup> provides an attractive alternative not containing the adjustable constant  $K$ . In the VFF model, the short-range energy due to stretching and bending of the bonds constitutes the enthalpy of mixing. This approach has been successfully used to calculate the enthalpy of mixing in III-V alloys without the adjustable parameter in the DLP model.<sup>27-31</sup>

As just mentioned, the DLP model always gives positive interaction parameters, which would suggest the occurrence of clustering and phase separation. Such phenomena are widely observed for III-V alloys.<sup>32,33</sup> However as mentioned in the Introduction section, ordering is also widely observed in semiconductor alloys. This apparent dilemma was anticipated in metal systems five decades ago by Hume-Rothery.<sup>34</sup> He recognized the obvious: that coherent clustering and phase separation—where the elastic energy at the boundary between regions with differing compositions is not allowed to relax via formation of defects such as dislocations—in systems with a large difference in atomic size gives rise to large macroscopic strain energies. He suggested that for such coherent systems a large size difference would drive both short- and long-range ordering rather than clustering. Thus he anticipated the observations in III-V alloys that both ordering and clustering can occur. Much more recent first-principle total-energy-minimization calculations by Zunger

and co-workers<sup>33</sup> led to the same conclusion. Ordering does reduce the total energy of random alloys composed of constituents that have a large lattice-parameter difference without producing a large macroscopic strain energy.

The first-principles calculations of Zunger and co-workers can be used to estimate the relative stabilities of the various ordered structures in III-V alloys.<sup>33</sup> For the bulk alloys—that is, ignoring surface effects—the CH ordered structure is found to be the most stable, followed closely by the CuAu structure.<sup>35</sup> The CuPt structure is not found to be stable relative to the disordered alloy. This was initially surprising since CuPt is nearly the only ordered structure observed experimentally. However this dilemma is resolved by considering the stabilities of the various ordered structures at the reconstructed surface.<sup>36</sup>

For the most commonly observed  $(2 \times 4)$  reconstruction on group-V-terminated (001) surfaces, recent VFF calculations<sup>36</sup> indicate that the B variants of the CuPt structure are the most stable. The [110] rows of  $\bar{1}\bar{1}0$ -oriented group-V dimers lead to alternating [110] rows of compressive and tensile strain in the third buried layer. For alloys with mixing on the group-III sublattice, such as GaInP, this produces the [110] rows of alternating large and small atoms that comprise the CuPt-B variants. These calculations also predict that the surface structure of alloys with mixing on the group-V sublattice, such as GaAsP, will also produce the CuPt-B variants, in agreement with experimental observations.<sup>37</sup>

**Effect of Growth Parameters on Ordering in GaInP**

The correspondence between the presence of  $\bar{1}\bar{1}0$  P dimers and CuPt ordering for GaInP layers grown by OMVPE has recently been verified by using the surface-photoabsorption (SPA) technique for measurement of the nature of the chemical bonding at the surface.<sup>38-40</sup> Optical techniques such as SPA are the only methods yielding *in situ* information about the surface reconstruction during OMVPE growth.<sup>41</sup> More direct techniques, such as reflection high-energy electron diffraction, are applicable only in ultrahigh-vacuum (UHV) systems. Optical techniques give information about only the energy and symmetry of electronic transitions involving surface atoms. Thus it is impossible to obtain information about the long-range order from such measurements. However SPA results correlate closely with RHEED results in UHV systems,<sup>42</sup> lending support to their use for determining indirectly the

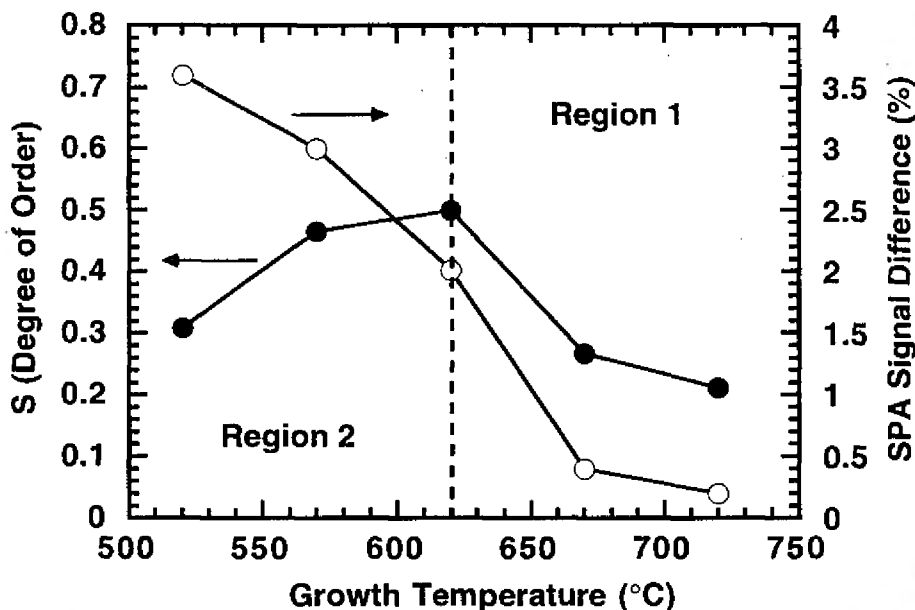


Figure 2. Degree of order and 400-nm surface-photoabsorption (SPA) signal due to  $\bar{1}\bar{1}0$  P dimers in GaInP versus temperature for growth at a tertiarybutylphosphine (TBP) partial pressure of 50 Pa.<sup>40</sup>

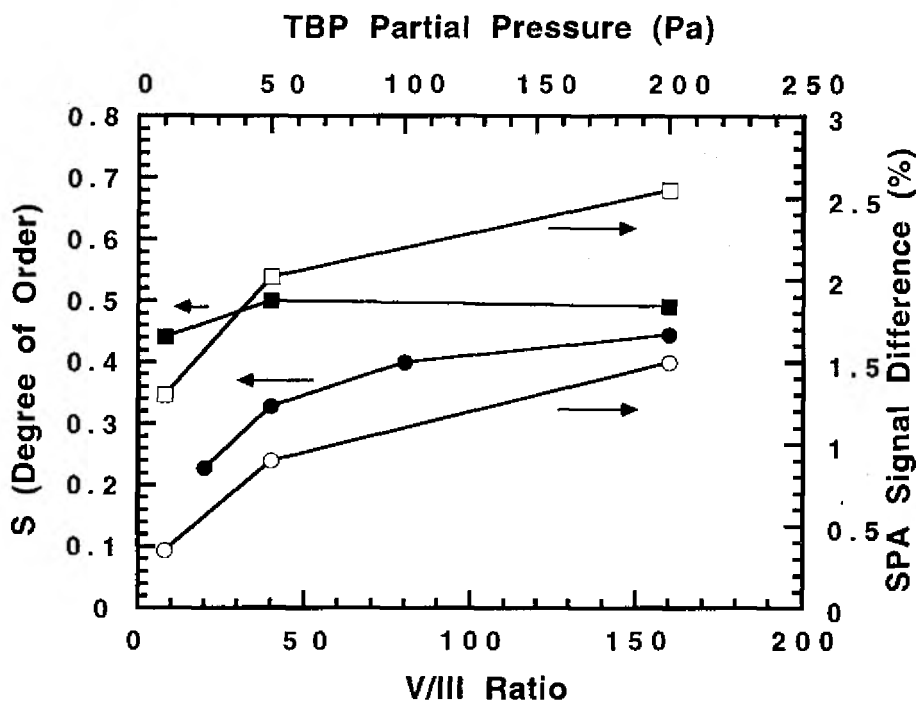


Figure 3. Degree of order and 400-nm SPA signal due to  $\bar{1}\bar{1}0$  P dimers versus the TBP partial pressure for growth at temperatures of 620°C (squares) and 670°C (circles).<sup>37</sup>

surface reconstruction during OMVPE growth. For example, the only known structures involving  $[110]$  group-V dimers on the (001) surface of III-V semiconductors are the  $(2 \times 4)$ -type reconstructions.

The effects of temperature during OMVPE growth on the degree of CuPt order has been studied extensively for GaInP. For example, a typical study using the reactants trimethylgallium, trimethylindium, and  $\text{PH}_3$ <sup>43</sup> shows a clear maximum in the degree of order at a temperature near 620°C, with a continuous decrease in order with increasing temperature until at 720°C the material is essentially disordered. Similarly a decrease in growth temperature to 520°C produces material with only a small degree of order. Nearly identical results were obtained by Murata et al.<sup>40</sup> for the OMVPE growth of GaInP using tertiarybutylphosphine (TBP) rather than phosphine, as Figure 2 shows.

Determining the concentration of  $[110]$  P dimers on the surface using SPA reveals that the major cause for the effect of temperature on ordering observed in GaInP grown by OMVPE is loss of the  $(2 \times 4)$ -like surface reconstruction providing the thermodynamic driving for ordering at the surface during growth. Figure 2 clearly demonstrates this, showing that the SPA signal intensity at 400 nm, due to the  $[110]$  P dimers, decreases sharply as the temperature increases from 620°C. At 720°C the signal has nearly disappeared.

However the data presented in Figure 2 make it very clear that the loss of order at low temperatures must be related to another factor. The SPA spectra for samples grown at low temperatures show a feature at approximately 480 nm that is attributed to an "excess phosphorus" phase; a second layer of P accumulates on the surface at low temperatures and high P partial pressures.<sup>44</sup> This may be the reason for the loss of CuPt order at low growth temperatures.

The flow rate of the group-V precursor is also found to have a significant effect on the ordering process. Again the degree of order has been closely correlated with the surface reconstruction.<sup>45</sup> In Figure 3, the degree of order is plotted versus the TBP partial pressure during growth at 620 and 670°C. The SPA intensity at 400 nm, due to the  $[110]$  P dimers, is also plotted. Clearly the loss of CuPt ordering at low V-III ratios correlates closely with the loss of the  $(2 \times 4)$ -like reconstruction.

The data from the studies of changing temperature and TBP partial pressure are combined for the plot of the degree of order versus the SPA signal in Figure 4.

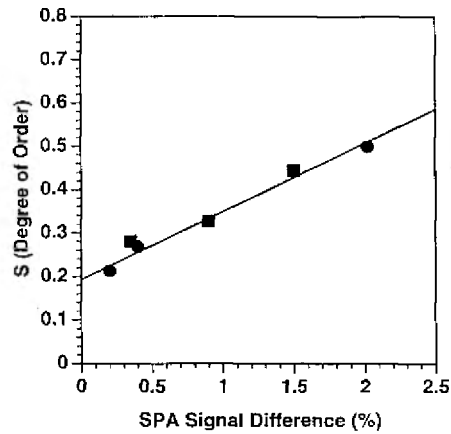


Figure 4. Degree of order versus SPA signal due to  $[110]$  P dimers for changing temperature (620–720°C) and changing TBP partial pressure (10–200 Pa).<sup>40</sup>

A one-to-one relationship between the degree of order and the concentration of  $[110]$  P dimers on the surface is observed for changes in both temperature (620–720°C) and TBP partial pressure (<200 Pa).

Support for the thermodynamic description of ordering is obtained from the results of annealing experiments. Plano et al.<sup>46</sup> were able to destroy the order produced in GaInP samples during growth by annealing for 4 h at 825°C. Similarly Gavrilovic et al.<sup>47</sup> were able to eliminate the ordered structure by annealing at 700°C for 100 h. This is evidence that the CuPt ordered structure is not stable in the bulk.

A strong link has clearly been established between the occurrence of CuPt ordering and the surface structure during growth. Both theoretical calculations and the results of experimental investigations strongly indicate that the CuPt structure is not stable in bulk GaInP. It forms at the surface during VPE growth on (001)-oriented substrates that are reconstructed to produce  $[110]$  rows of  $[110]$  group-V dimers on the surface.

However other factors are also found to affect ordering and are related to the mechanism responsible for ordering. For example, misorientation of the (001) substrates by a few degrees to produce  $[110]$  surface steps is found to enhance the formation of the CuPt ordered structure while  $[110]$  steps are found to retard the ordering process. This suggests that surface steps may play an important role in the kinetic processes leading to the formation of the CuPt ordered structure.

The results of growth-rate studies also

strongly suggest that other, kinetic factors may be significant in the ordering process. Considering only thermodynamic factors, the growth rate should not affect the ordering in GaInP for OMVPE growth at high V-III ratios. Changing the partial pressures of the Ga and In precursors will change the growth rate but will not affect the P partial pressure at the interface.<sup>25</sup> Thus the P coverage of the surface and the surface reconstruction should be independent of growth rate. In recent experiments at a temperature of 670°C, the group-III flow rates were changed while the TBP partial pressure remained constant at 1.5 Torr. Changing the growth rate from 0.25 to 2  $\mu\text{m}/\text{h}$  was found to have no detectable effect on the degree of order.<sup>48</sup> This clearly demonstrates the lack of a kinetic factor in the ordering process under these conditions. However at higher growth rates, a kinetic factor becomes clearly evident. Cao et al.<sup>49</sup> studied the effect of growth rate on ordering in GaInP grown by OMVPE at rates from 4 to 12  $\mu\text{m}/\text{h}$  at a temperature of 680°C. They found a marked decrease in the degree of order at the higher growth rates. The ordering is virtually eliminated at a growth rate of 12  $\mu\text{m}/\text{h}$  (about 10 monolayers/s). The reduction in order parameter with increasing growth rate seen for rates above 4  $\mu\text{m}/\text{h}$  gives a rough measure of the rate of the ordering process occurring on the surface during growth. The data indicate that the time constant is approximately 0.25 s. Cao et al. attributed this to surface diffusion. This mechanism would be consistent with a time constant of this magnitude. Several authors have suggested a subsurface diffusion model to account for ordering.<sup>10,33,50</sup> However it seems highly unlikely that subsurface diffusion could occur at a rate consistent with this time constant. It would require a diffusion coefficient in the solid many orders of magnitude higher than the bulk diffusion coefficients measured in III-V systems.

## Summary

The phenomenon of atomic-scale ordering during the VPE growth process to produce natural monolayer superlattices was discovered in III-V alloys a little over a decade ago. During the intervening years, the CuPt ordered structure with ordering on  $\{111\}$  planes has been found to occur in virtually all III-V semiconductors for growth on the (001) plane. Both theory and experimental results indicate that the CuPt structure is not thermodynamically stable in the bulk alloys. It is stabilized by the formation of  $[110]$  rows of  $[110]$  dimers on the surface during growth. The subsurface lattice sites

are in compression directly below the dimers and in tension between the dimers. This leads to the arrangement of the Ga and In atoms in GaInP, for example, into the alternating [110] rows that comprise the B variants of the CuPt structure with ordering on ( $\bar{1}11$ ) and ( $1\bar{1}1$ ) planes. A direct link between formation of the CuPt structure and the concentration of [ $\bar{1}10$ ] P dimers, when changing either the temperature or the partial pressure of the P precursor, now has been established using SPA to measure the dimer concentration. However other factors also affect ordering. CuPt order disappears for low growth temperatures. This is found to correlate with appearance of an excess P phase where a second layer of P is formed on the surface. Evidence of the role of surface steps is the enhancement of ordering by [110] steps and diminution of ordering when [ $\bar{1}10$ ] steps are introduced. This strongly indicates that the step structure also plays a role in the ordering process, as it ultimately must since this is where all adatoms are incorporated into the lattice. Examination of the effect of growth rate gives some idea of the kinetics of the ordering process. At rates above 4  $\mu\text{m/h}$ , the ordering weakens and almost disappears at a growth rate of 12  $\mu\text{m/h}$ . This indicates that the kinetics of the ordering process are relatively rapid, probably too rapid to be a subsurface diffusion process occurring in the third layer below the surface, as suggested by some models. At this time, we have no compelling model to explain the effects of steps on the ordering process.

One reason that ordering has received so much attention is because the bandgap energy is strongly dependent on the CuPt order parameter. Theoretical and experimental studies indicate that the bandgap energy of completely ordered GaInP will be 300–500 meV less than for disordered material. For this reason, order must be strictly controlled for materials used for both electronic and photonic devices. We are now beginning to explore the use of ordering to improve the performance of devices.

### Acknowledgments

I wish to express my appreciation to the Department of Energy and the National Science Foundation for supporting

my fundamental studies of ordering in III-V semiconductors.

### References

1. T.S. Kuan, T.F. Kuech, W.I. Wang, and E.L. Wilkie, *Phys. Rev. Lett.* **54** (1985) p. 201.
2. H.R. Jen, M.J. Cherng, and G.B. Stringfellow, *Appl. Phys. Lett.* **48** (1986) p. 1603.
3. H. Nakayama and H. Fujita, *Inst. Phys. Conf. Ser.* **79** (1986) p. 289.
4. I.J. Murgatroyd, A.G. Norman, and G.R. Booker, *J. Appl. Phys.* **67** (1990) p. 2310.
5. T.S. Kuan, W.I. Wang, and E.L. Wilkie, *Appl. Phys. Lett.* **51** (1987) p. 51.
6. G.B. Stringfellow and G.S. Chen, *J. Vac. Sci. Technol. B* **9** (1991) p. 2182.
7. S.-H. Wei and Z. Zunger, *Phys. Rev. B* **39** (1989) p. 3279.
8. K.E. Newman, J. Shen, and D. Teng, *Superlattices and Microstructures* **6** (1989) p. 245.
9. K. Park, L. Salabanca-Riba, and B.T. Jonker, *Appl. Phys. Lett.* **61** (1992) p. 2302; L. Salabanca-Riba, K. Park, and B.T. Jonker, in *Magnetic Surfaces, Thin Films, and Multilayers*, edited by S.S.P. Parkin, H. Hopster, J.-P. Renard, T. Shinjo, and W. Zinn (Mater. Res. Soc. Symp. Proc. **231**, Pittsburgh, 1992) p. 347; K.T. Chang and E. Goo, *J. Vac. Sci. Technol. A* **10** (1992) p. 1549.
10. F.K. LeGoues, V.P. Kesan, and S.S. Iyer, *Phys. Rev. Lett.* **64** (1990) p. 40.
11. L.C. Su, I.H. Ho, and G.B. Stringfellow, *J. Appl. Phys.* **75** (1994) p. 5135.
12. D. Mao, P.C. Taylor, S.R. Kurtz, M.C. Wu, and W.A. Harrison, *Phys. Rev. Lett.* **76** (1996) p. 4769.
13. S.-H. Wei and A. Zunger, *Phys. Rev. B* **49** (1994) p. 14337.
14. T.Y. Seong, G.R. Booker, A.G. Norman, P.J.F. Harris, and A.G. Cullis, *Inst. Phys. Conf. Ser.* **146** (1995) p. 241; T.Y. Seong, A.G. Norman, G.R. Booker, and A.G. Cullis, *J. Appl. Phys.* **75** (1994) p. 7852.
15. G.B. Stringfellow, P.F. Lindquist, and R.A. Burmeister, *J. Electron. Mater.* **1** (1972) p. 437.
16. A. Gomyo, K. Iobayashi, S. Kawata, I. Hino, T. Suzuki, and T. Yuasa, *J. Cryst. Growth* **77** (1986) p. 367.
17. S.-H. Wei, A. Franceschetti, and A. Zunger, in *Ion Beam Processing of Advanced Electronic Materials*, edited by N.W. Cheung, A.D. Marwick, and J.B. Roberto (Mater. Res. Soc. Symp. Proc. **417**, Pittsburgh, 1989) p. 3.
18. D.B. Laks, S.-H. Wei, and A. Zunger, *Phys. Rev. Lett.* **69** (1992) p. 3766.
19. P. Ernst, C. Geng, F. Scholz, H. Schweizer, Y. Zhang, and A. Mascarenhas, *Appl. Phys. Lett.* **67** (1995) p. 2347.
20. D.J. Arent, M. Bode, K.A. Bertness, S.R. Kurtz, and J.M. Olson, *ibid.* **62** (1993) p. 1806.
21. S.R. Kurtz, L.R. Dawson, R.M. Biefeld, D.M. Follstaedt, and B.L. Doyle, *Phys. Rev. B* **46** (1992) p. 1909.
22. L.C. Su, I.H. Ho, and G.B. Stringfellow, *J. Cryst. Growth* **145** (1994) p. 140.
23. G.B. Stringfellow, *J. Phys. Chem. Solids* **33** (1972) p. 665.
24. *Ibid.*, *J. Cryst. Growth* **27** (1974) p. 21.
25. *Ibid.*, *Organometallic Vapor Phase Epitaxy: Theory and Practice*, ch. 3 (Academic Press, Boston, 1989).
26. P.N. Keating, *Phys. Rev.* **145** (1966) p. 637.
27. T. Fukui, *J. Appl. Phys.* **57** (1985) p. 5188.
28. M. Ichimura and A. Sasaki, *J. Cryst. Growth* **98** (1989) p. 18.
29. M.C. Schabel and J.L. Martins, *Phys. Rev. B* **43** (1991) p. 11873.
30. A. Sher, M. van Schilfgaarde, A.B. Chen, and W. Chen, *ibid.* **36** (1987) p. 4279.
31. I.H. Ho and G.B. Stringfellow, *Appl. Phys. Lett.* **69** (1996) p. 2701.
32. G.B. Stringfellow, *J. Cryst. Growth* **98** (1989) p. 108.
33. A. Zunger and S. Mahajan, in *Handbook on Semiconductors*, edited by T.S. Moss (Elsevier Science B.V., Amsterdam, 1994) p. 1399.
34. W. Hume-Rothery, *Electrons, Atoms, Metals, and Alloys*, 3rd ed. (Dover, New York, 1963). The first edition was published in 1948.
35. J.E. Bernard, R.G. Dandrea, L.G. Ferreira, S. Froyen, S.-H. Wei, and A. Zunger, *ibid.* **56** (1990) p. 731.
36. S.B. Zhang, S. Froyen, and A. Zunger, *ibid.* **67** (1995) p. 3141.
37. G.S. Chen, D.H. Jaw, and G.B. Stringfellow, *J. Appl. Phys.* **69** (1991) p. 4263.
38. H. Murata, I.H. Ho, T.C. Hsu, and G.B. Stringfellow, *Appl. Phys. Lett.* **67** (1995) p. 3747.
39. H. Murata, T.C. Hsu, I.H. Ho, L.C. Su, Y. Hosokawa, and G.B. Stringfellow, *ibid.* **68** (1996) p. 1796.
40. H. Murata, I.H. Ho, L.C. Su, Y. Hosokawa, and G.B. Stringfellow, *J. Appl. Phys.* **79** (1996) p. 6895.
41. Y. Kobayashi and N. Kobayashi, *J. Electron. Mater.* **25** (1996) p. 691.
42. I. Kamiya, L. Mantese, D.E. Aspnes, D.W. Kisker, P.H. Fuoss, G.B. Stephenson, and S. Brennan, *J. Cryst. Growth* **163** (1996) p. 67.
43. L.C. Su, I.H. Ho, and G.B. Stringfellow, *ibid.* **146** (1995) p. 558.
44. H. Murata, I.H. Ho, and G.B. Stringfellow, *ibid.* **ICMOVPE-96**.
45. H. Murata, S.H. Lee, I.H. Ho, and G.B. Stringfellow, *J. Vac. Sci. Technol. B* **14** (1996) p. 3013.
46. W.E. Plano, D.W. Nam, J.S. Major, K.C. Hsieh, and N. Holonyak, *Appl. Phys. Lett.* **53** (1988) p. 2537.
47. P. Gavriloic, F.P. Dabkowski, K. Meehan, J.E. Williams, W. Statius, K.C. Hsieh, N. Holonyak, M.A. Shahid, and S. Mahajan, *J. Cryst. Growth* **93** (1988) p. 426.
48. Y.S. Chun, S.H. Lee, I.H. Ho, and G.B. Stringfellow, *J. Appl. Phys.* in press.
49. D.S. Cao, E.H. Reihlen, G.S. Chen, A.W. Kimball, and G.B. Stringfellow, *J. Cryst. Growth* **109** (1991) p. 279.
50. B.A. Philips, A.G. Norman, T.Y. Seong, S. Mahajan, G.R. Booker, M. Skowronski, J.P. Harbison, and V.G. Keramidis, *ibid.* **140** (1994) p. 249. □

Materials Research  
Society Website

<http://www.mrs.org/>

- Meetings
- Membership
- Publications